Spatiotemporal Hierarchy of Relaxation Events, Dynamical Heterogeneities, and Structural Reorganization in a Supercooled Liquid

R. Candelier,[1] A. Widmer-Cooper,[2] J. K. Kummerfeld,[3] O. Dauchot,[1] G. Biroli,[4] P. Harrowell,[3] and D. R. Reichman[5]

[1]*SPEC, CEA-Saclay, URA 2464 CNRS, 91 191 Gif-sur-Yvette, France*
[2]*Materials Sciences Division, Lawrence Berkeley National Laboratory, Berkeley, California, 94720, USA*
[3]*Department of Chemistry, University of Sydney, Sydney, New South Wales 2006, Australia*
[4]*Institut de Physique Théorique, CEA, IPhT, F-91191 Gif-sur-Yvette, France and CNRS, URA 2306*
[5]*Columbia University, 3000 Broadway, New York, New York, 10027, USA*

We identify the pattern of microscopic dynamical relaxation for a two-dimensional glass-forming liquid. On short time scales, bursts of irreversible particle motion, called cage jumps, aggregate into clusters. On larger time scales, clusters aggregate both spatially and temporally into avalanches. This propagation of mobility takes place along the soft regions of the systems, which have been identified by computing isoconfigurational Debye-Waller maps. Our results characterize the way in which dynamical heterogeneity evolves in moderately supercooled liquids and reveal that it is astonishingly similar to the one found for dense glassy granular media.

Identifying the mechanisms responsible for the slowing down of the dynamics of supercooled liquids is still an open problem despite decades of research. While traditional descriptions of glassy systems have mainly focused on energy landscape concepts [1] and spatially averaged quantities, recent work has centered on the real-space properties reflected in the heterogeneous dynamics shown by nearly all glass-forming materials. Concomitantly, investigations of the behavior of dense driven granular media have uncovered tantalizing similarities with the dynamics of supercooled liquids [2–5] and provided new inspirations for research on the glass transition. One notable finding from the granular studies is that dynamic heterogeneities are organized into a hierarchy of structures, each of them characterized by its length and time scales [6,7]. Cage escapes by individual particles occur in clusters which, in turn, are organized into larger collections that were called "avalanches," referring to large collective events composed sequentially by smaller ones.

An important question is whether this hierarchy of dynamic heterogeneities is present in thermally equilibrated supercooled liquids or, instead, it is a peculiarity of athermal dissipative systems. Evidence of organized motion in liquids has already been reported [8–12]: on relatively fast time scales, the complex sequence of particle motions results in stringlike clusters of displacements, see, e.g., [10]; on time scales on which relaxation takes place, particle motion is organized in compact clusters [11]. While these studies are encouraging, neither the extended spatial hierarchy of particle escape within clusters and avalanches nor how the dynamical correlations form starting from microscopic time scales out to the structural relaxation time have been explored. In this Letter we identify these mechanisms and demonstrate that the dynamic heterogeneities of a supercooled liquid are, in fact,

organized in an hierarchy essentially identical to that found in granular systems.

Understanding how the spatial distribution of kinetics arises from the structure of the underlying particle configurations represents a central challenge for any complete discussion of a glass transition. We therefore also investigate how this hierarchy of length and time scales is expressed in the configurational structure. Using the isoconfigurational ensemble and the local Debye-Waller (DW) factor, correlations between structure and dynamic heterogeneities have been established [13,14]. Here we show mechanistically and in detail how clusters and avalanches develop on soft regions of the structure and, inversely, how these relaxation events change the spatial distribution of the soft regions.

We shall address these questions by performing molecular dynamics simulations on a new two-dimensional model of glass-forming liquid and applying the cluster analysis developed in [6]. We focus on a 2D nonadditive binary mixture of $N = 5760$ particles enclosed in a square box with periodic boundary conditions, interacting via purely repulsive potentials of the form $u_{ab}(r) = \varepsilon(\sigma_{ab}/r)^{12}$. The mole fraction of the smaller particles is set to $x_1 = 0.3167$. All units are reduced so that $\sigma_{11} = \varepsilon = m = 1.0$, m being the mass of both types of particle. The nonadditivity potential, namely, $\sigma_{12} = 1.1\sigma_{11}$ and $\sigma_{22} = 1.4\sigma_{11}$, hinders the formation of crystalline microdomains; see [15] for more details. Molecular dynamics simulations were carried out at constant NVT ($T = 0.4$) using the Nose-Poincaré Hamiltonian [16] after equilibration at constant NPT as described in [14]. All time units are scaled in such a way that the structural relaxation time τ_α, defined as the time required for the self-intermediate scattering function to decay to $1/2$, equals 10^3. The typical collision time is 0.12 in these units.

To compare the dynamic heterogeneities of the simulated liquid and granular system we quantify the local relaxation of a particle p by

$$Q_{p,t}(a, \tau) = \exp\left(-\frac{\|\Delta\vec{r}_p(t, t+\tau)\|^2}{2a^2}\right), \qquad (1)$$

where $\Delta\vec{r}_p(t, t+\tau)$ is the displacement of the particle p between t and $t+\tau$ and a is the length scale over which the motion is probed. A global measure of the relaxation is then provided by the correlation function, $Q_t(a, \tau) = \frac{1}{N}\sum_p Q_{p,t}(a, \tau)$, and its fluctuations $\chi_4(a, \tau) = N \operatorname{Var}[Q_t(a, \tau)]$. We focus on the values $a^* = 0.29$ and $\tau^* = 1078$ leading to maximal dynamic heterogeneity, i.e., highest value of $\chi_4(a, \tau)$ (see [17] for details). Note that τ^* is very close to the relaxation time $\tau_\alpha = 1000$.

To define cage jumps, we follow the same procedure as in [6]. Briefly, the trajectory of each particle is divided in two at a time t_c, t_c being chosen such that the centers of mass of the subtrajectories on either side of t_c are best separated. t_c is designated a cage escape, and the process is repeated iteratively for each of the subtrajectories until the maximal separation drops below a threshold distance stemming from the dynamics itself. This allows one to separate the dynamics into periods of inefficient vibrational motion separated by relaxation events also called cage jumps (see inset of the top-left panel of Fig. 1). Note that a particle undergoing a cage jump does not necessarily change neighbors, since the typical jump distance is well below the particle size. The relative percentage of particles that have not jumped matches perfectly the temporal evolution of the dynamical relaxation (Fig. 1, top left) and the location of the cage jumps coincides with the areas of maximal decorrelation (Fig. 1, top right).

Figure 1 (top right) already suggests some level of spatiotemporal organization of the cage jumps. This can be further quantified following the analysis performed for the two-dimensional granular media [6]. The outcome is remarkably similar (Fig. 1, bottom right): First, cage jumps aggregate into clusters, which are formed by cage jumps adjacent in space (as measured by the neighboring particles) and time (separated by less than $\tau_{th} = 28$, which is twice the precision of the cage detection algorithm). The size of these clusters is broadly distributed with an average value of 7.6 cage jumps per cluster. Second, clusters aggregate into avalanches. The probability distribution function (PDF) of the lag times τ_1 separating each cluster from the nearest adjacent one, normalized by its average value $\langle\tau_1\rangle$, is compared to the equivalent distributions for randomly distributed clusters in space and time (Fig. 1, bottom left). There is a clear excess of both small and large lags: the PDF is very well fitted by the superposition of two Poissonian processes with two different time scales $\tau_S = 240$ and $\tau_L = 1746$. The short time scale corresponds to the existence of a correlation among adjacent clusters. The large one is related to the average time spent in a cage. Table I compares the actual values of these parameters to
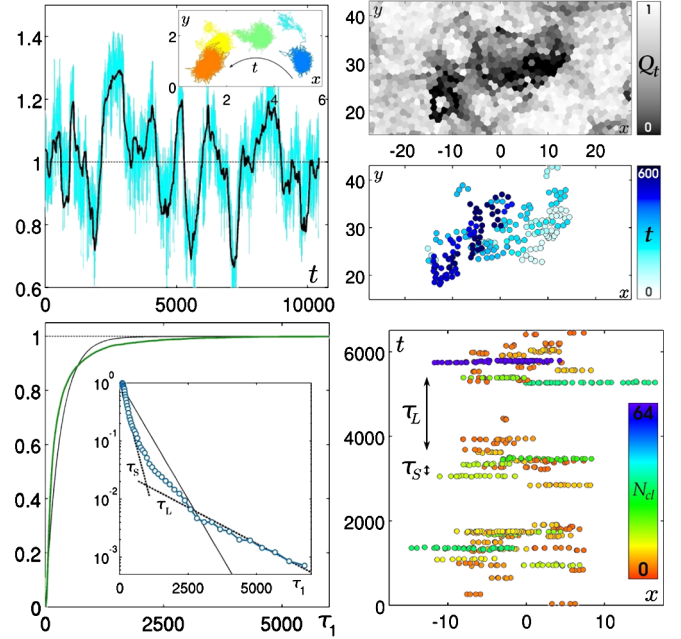

FIG. 1 (color online). Cage jump spatiotemporal organization. Top left: Comparison between the relative averaged relaxation $Q_t(a^*, \tau^*)/\langle Q_t\rangle_t$ [gray (cyan)] and the relative percentage $P_t(\tau^*)/\langle P_t\rangle_t$ of particles that have not jumped between t_0 and $t_0 + \tau^*$ (black). Inset: Trajectory of a single particle over $14\tau_\alpha$. Color changes when the particle jumps. Top right: (inner top) Map of $Q_{t_0}(\tau^*)$; (inner bottom) particles having jumped during the same lag τ^*; jumping time is color-coded. Bottom left: Cumulative probability distribution function of the lag between adjacent clusters τ_1 (thick green curve), compared to the corresponding curve for a random distribution of clusters (black). Inset: PDF of τ_1 (circles). The exponential distribution with same mean is shown for comparison (solid line), as well as exponentials of typical time scale τ_S and τ_L (dotted lines). Bottom right: Spatiotemporal view of the cage jumps in a specific region of space, projected on the x axis. The cluster size is color-coded. Note the aggregation of clusters in avalanches. The typical time scales of the dynamics are shown.

those of the granular system investigated previously. We also report the value of the dynamical correlation length ξ_4, obtained from the spatial range of the dynamical correlator G_4 computed at τ^*; see, e.g., [18]. The dynamics are strikingly similar. One difference we find is that the average distance between avalanches is somewhat smaller in the liquid case than in the granular one: ~ 10 as compared to ~ 27. More evidence, as well as details on the procedure for identifying cage jumps and analyzing them, are reported in the supplementary material [19].

TABLE I. Comparison of length and time scales normalized so that $\tau_\alpha = 1000$. See definitions in the text.

	a^*	ξ_4	τ_α	τ^*	τ_S	τ_L
Supercooled liquid	0.29	2.9	1000	1078	240	1746
Dense granular media	0.12	3.1	1000	915	155	1384

Altogether, this first part of our study clearly demonstrates that the nature of dynamic heterogeneity in supercooled and granular systems is largely the same, a nontrivial result given the difference between an equilibrated thermal liquid and a nonequilibrium steady state of vibrated grains. Recent results [7] obtained by changing the density of the granular sample suggest that our model of a supercooled liquid would compare with a granular system characterized by a slightly smaller density than the one studied here. Obviously the next step is to perform a careful study of the temperature dependence, which will require significant further supercooling.

The existence of avalanches is consistent with a scenario in which the first cluster triggers the appearance of successive clusters nearby shortly after. This is reminiscent of the facilitation picture inspired from facilitated kinetic Ising models, for which mobility diffuses as a locally conserved quantity [20,21]. However, in a real system, there should always be a probability to create or annihilate a facilitated chain of motion and facilitation is not fully conserved. This is precisely what we see when avalanches start or end. As compared to other studies of supercooled liquids, we believe that the democratic clusters [10] correspond with the avalanches.

We shall now address how (if at all) this organization of dynamics is reflected in the structure of the relevant configuration. Here we will identify the location of "soft" regions by using the isoconfigurational DW factor [14,22]. Starting from the system configuration at time t, one computes the local DW factor for particle i: $(\mathrm{DW})_i = \langle[\vec{r}_i(t) - \langle\vec{r}_i\rangle_{\delta t}]^2\rangle_{\delta t, \mathcal{C}}$, where the average is over the isoconfiguration ensemble as well as over a short time interval δt which in this work is taken to be 25. Starting from the same equilibrated configuration, we have run 6 isotrajectories and have obtained the cage jumps for all of them.

All of the cage jumps occurring in the interval of time $[t, t + \tau_S]$ fall on top of high DW areas; see Fig. 2, top. However, when and where the clusters exactly appear is a stochastic event. Note that $\tau_S \gg 25$, so that the correlation between the DW map at time t (a nearly instantaneous structural quantity) and the dynamics taking place at longer times are nontrivial. The correlation between DWs and cage jumps can be made more quantitative. We compute the DW at time t averaged only over particles that jump between t and $t + \tau$ (DW^J) as a function of the lag time τ. This quantity, normalized with respect to $\langle\mathrm{DW}(t)\rangle_t$ for all particles, is shown in Fig. 2 (bottom right). At short times the average $(\mathrm{DW})^J$ for the jumping particles is substantially higher than the DW averaged over all particles. This correlation disappears for larger times comparable to times over which the DW maps decorrelate, which is of the order of $\tau_\alpha/3$.

If we consider now the sequence of multiple clusters, as shown in the two top panels of Fig. 2, we find strong evidence that a significant part of the avalanche structure, not just the initial cluster in an avalanche, lies on top of the
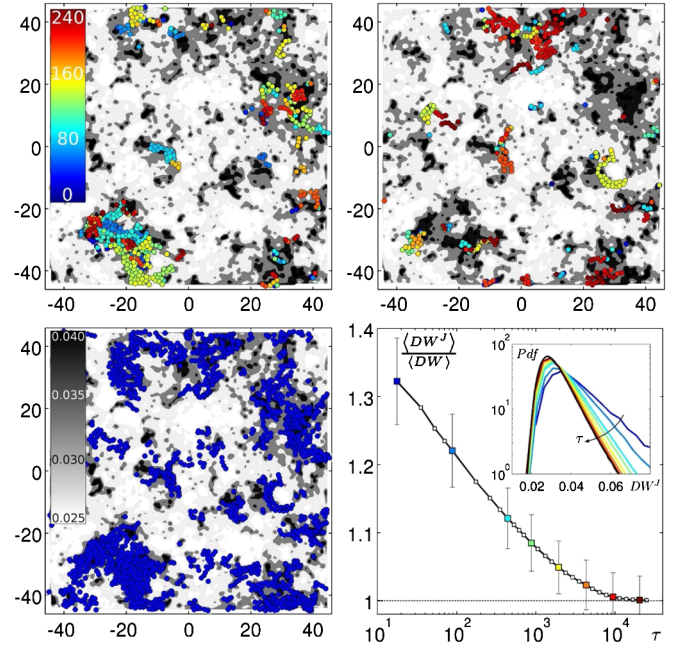

FIG. 2 (color online). Top: Cage jumps occurring between t and $t + \tau_S$ for two different isoconfigurational trajectories, on top of a DW factor map computed at time t. Bottom left: Cage jumps occurring in 6 isoconfigurational trajectories between t and $t + \tau_S$ tile the high DW regions. Color bar indicates the DW values in levels of gray. Bottom right: Average $\langle(\mathrm{DW})^J\rangle$ over the particles having jumped between t and $t + \tau$, divided by the average $\langle\mathrm{DW}\rangle$ over all particles, as a function of the lag time τ. Inset: PDF of $(\mathrm{DW})^J$ for the particles jumping in $[t; t + \tau]$ for several values of τ. The black curve is the PDF for all particles.

real-space geometric structure encoded in the soft regions. Remarkably, merging all cage jumps that occur in the interval of time τ_S in the 6 isoconfigurational trajectories covers nearly all the high DW areas, as shown in Fig. 2 (bottom left). Our conclusion is that the spatial distribution of soft regions encoded in the initial configuration provides a better predictor of the avalanche than for its constitutive clusters. This result is consistent with the previous conclusion of Berthier and Jack [23], who found that structural properties are better predictors of dynamics on large as opposed to short length scales.

We finally consider an issue never addressed before, namely, how the dynamics causes the soft regions of the structure to evolve. We find that decorrelation is a distinctly nonlocal process. More precisely, a cage jump at time t correlates with changes of the DWs that happen shortly after and extend quite far away. This is visually apparent in Fig. 3 (left) and demonstrated quantitatively by considering $|\mathrm{DW}(t) - \mathrm{DW}(t + \tau)|$ averaged over all particles, that are in a disk of radius r from a cage jump taking place at time t and subtract from that quantity its $r = \infty$ value. Figure 3 (right) shows this quantity, called $\Delta^J(r)$, for $\tau = 17$. $\Delta^J(r)$ is rather long ranged, in particular, much more than the cage jump correlation function $\rho^J(r)$; see Fig. 3 (right) and its caption for a precise definition of
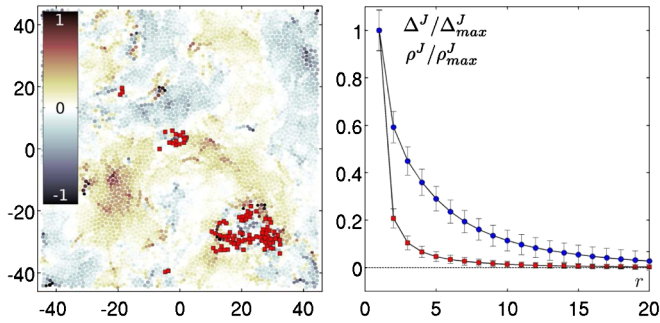
FIG. 3 (color online). Left: Cage jumps occurring in $\tau = 17$ on top of a map of the relative difference $(DW(t+\tau) - DW(t))/\langle DW \rangle$. Right: Normalized $\Delta^J(r) = \langle |\delta(DW)_i| \rangle_r^J - \langle |\delta(DW)_i| \rangle_\infty^J$ (blue circles) where $\langle |\delta(DW)_i| \rangle_r^J$ is the absolute difference of DW over $\tau = 17$ averaged over the particles in the disk of radius r around a given cage jump. The analogous quantity for the density of jumps $\rho^J(r) = \langle \delta_i \rangle_r^J - \langle \delta_i \rangle_\infty^J$ (red squares) where δ_i is 1 if particle i jumps between t and $t+\tau$ and 0 otherwise. Error bars: standard deviation.

$\rho^J(r)$. What is mediating the nonlocal interaction between cage jumps and DWs is an intriguing question. One possibility is that a slowly varying spatial field, like the thermal strain discussed in [12], provides long-ranged dynamical interactions.

In conclusion, we have established that the organization of cage jumps into clusters and avalanches, observed originally in the driven granular system in [6,7], also characterizes the dynamic heterogeneities of a simulated supercooled liquid, at least away from deep supercooling. This demonstration of the existence of avalanches in supercooled liquids suggests that there is a hierarchy of lengths related to the cooperative dynamics. The irrelevance of the very different types of particle dynamics in the two systems possibly is a consequence of the dominant role played by structure in the dynamics of these dense disordered systems. The spatial extent of the avalanches is strongly correlated with the extent of the spatial regions of large local DW factors. This result raises the possibility that the hierarchy of kinetic length, mentioned above, may have a corresponding hierarchy in the inherent structures of glass-forming liquids. The importance of the preexisting soft modes in determining the structure of dynamic heterogeneities and the nonlocal influence on the evolution of the topography of hard and soft areas leaves us with a quite different view from the one based on the propagation of a conserved mobility field.

Studying the evolution of dynamical properties with decreasing temperature following the same analysis would allow for direct tests of prominent theories of the glass transition. In the picture based on kinetically constrained models of glasses [21], facilitation should become more relevant and conserved upon lowering the temperature. In the random first order transition theory [24], the dynamics should be correlated with soft regions for moderately supercooled liquids, but, closer to the glass transition, the relaxation should be dominated by other processes. Three of us [7] have performed such an analysis for granular media and found that facilitation becomes *less* conserved as the density is increased. A similar analysis for our model of supercooled liquids is in progress.

[1] M. Goldstein, J. Chem. Phys. **51**, 3728 (1969).
[2] G. Marty and O. Dauchot, Phys. Rev. Lett. **94**, 015701 (2005).
[3] A. R. Abate and D. J. Durian, Phys. Rev. E **74**, 031308 (2006).
[4] C. S. O'Hern, S. A. Langer, A. J. Liu, and S. R. Nagel, Phys. Rev. Lett. **88**, 075507 (2002).
[5] A. Liu and S. Nagel, Nature (London) **396**, 21 (1998).
[6] R. Candelier, O. Dauchot, and G. Biroli, Phys. Rev. Lett. **102**, 088001 (2009).
[7] R. Candelier, O. Dauchot, and G. Biroli, arXiv:0912.0472.
[8] R. Yamamoto and A. Onuki, J. Phys. Soc. Jpn. **66**, 2545 (1997).
[9] C. Donati, S. C. Glotzer, P. H. Poole, W. Kob, and S. J. Plimpton, Phys. Rev. E **60**, 3107 (1999).
[10] Y. Gebremichael, M. Vogel, and S. C. Glotzer, J. Chem. Phys. **120**, 4415 (2004).
[11] G. A. Appignanesi, J. A. Rodriguez Fris, R. A. Montani, and W. Kob, Phys. Rev. Lett. **96**, 057801 (2006).
[12] A. Widmer-Cooper and P. Harrowell, Phys. Rev. E **80**, 061501 (2009).
[13] A. Widmer-Cooper, P. Harrowell, and H. Fynewever, Phys. Rev. Lett. **93**, 135701 (2004).
[14] A. Widmer-Cooper, H. Perry, P. Harrowell, and D. R. Reichman, Nature Phys. **4**, 711 (2008).
[15] A. Widmer-Cooper, Ph.D. thesis, University of Sydney, 2006.
[16] S. D. Bond, B. J. Leimkuhler, and B. B. Laird, J. Comput. Phys. **151**, 114 (1999).
[17] F. Lechenault, O. Dauchot, G. Biroli, and J. Bouchaud, Europhys. Lett. **83**, 46003 (2008).
[18] S. Glotzer, V. Novikov, and T. Schrøder, J. Chem. Phys. **112**, 509 (2000).
[19] See supplementary material at http://link.aps.org/supplemental/10.1103/PhysRevLett.105.135702 for details.
[20] S. Butler and P. Harrowell, J. Chem. Phys. **95**, 4454 (1991).
[21] J. P. Garrahan and D. Chandler, Phys. Rev. Lett. **89**, 035704 (2002).
[22] A. Widmer-Cooper and P. Harrowell, Phys. Rev. Lett. **96**, 185701 (2006).
[23] L. Berthier and R. L. Jack, Phys. Rev. E **76**, 041509 (2007).
[24] T. R. Kirkpatrick, D. Thirumalai, and P. G. Wolynes, Phys. Rev. A **40**, 1045 (1989).